Bis(diphenylphosphino)acetylene as Bifunctional Ligand in Dicobalt Carbonyl Complexes

Fung-E Hong,* Yu-Chang Chang, Ruei-E Chang, Shu-Chun Chen, and Bao-Tsan Ko

Department of Chemistry, National Chung-Hsing University, Taichung 40227, Taiwan

Received July 27, 2001

Treatment of bis(diphenylphosphino)acetylene (DPPA) with a bis(diphenylphosphino)-methylene (DPPM)-bridged dicobalt complex, [{μ-P,P-$PPh_2CH_2PPh_2$}$Co_2(CO)_6$], **3**, yielded a DPPA-bridged dicobalt compound, [{μ-P,P-$PPh_2CH_2PPh_2$}$Co_2(CO)_4${μ-$PPh_2C{\equiv}CPPh_2$}], **5**. Two oxidized complexes, [{μ-P,P-$PPh_2CH_2PPh_2$}$Co_2(CO)_4${μ-$PPh_2C{\equiv}CP(=O)Ph_2$}], **6**, and [{μ-P,P-$PPh_2CH_2PPh_2$}$Co_2(CO)_4${μ-$P(=O)Ph_2C{\equiv}CP(=O)Ph_2$}], **7**, were obtained along with **5** during the chromatographic separation process. Further reaction of **5** with selenium powder in THF at 25 °C produced [{μ-P,P-$PPh_2CH_2PPh_2$}$Co_2(CO)_4${μ-$P(=O)Ph_2C{\equiv}CP(=Se)Ph_2$}], **8**, a compound with two phosphorus atoms of **5** oxidized by oxygen and selenium, respectively. The $^{31}P-^{77}Se$ coupling constant of the Se−P bond is 723 Hz. The reaction of **5** with $Mo(CO)_6$ in toluene at 110 °C yielded [{μ-P,P-$PPh_2CH_2PPh_2$}$Co_2(CO)_4${μ-P,P-$PPh_2C{\equiv}CPPh_2$}$Mo(CO)_4$], **9**. Compounds **5**−**9** were characterized by spectroscopic means as well as by X-ray diffraction studies. Crystal structures of **6**−**8** reveal that the distance between the oxide and the adjacent methylene proton is within the range of an intramolecular hydrogen bond. The structure of **9** reveals that **5** behaves as a diphosphine chelating ligand toward the $Mo(CO)_4$ fragment. The fluxional behavior of the DPPM ligands in **5** and **9** were examined by variable-temperature ^1H NMR experiments. The calculated activation energies for the fluxional processes are 19.2 and 7.1 kcal/mol for **5** and **9**, respectively.

Introduction

Bidentate phosphine ligands have played an important role in transition metal-based homogeneous catalysis.[1] Recently, the capacity of bis(diphenylphosphino)-acetylene ($PPh_2C{\equiv}CPPh_2$) to act as a bifunctional ligand to transition metals has been examined widely.[2]

Our previous work described the preparation of one type of bidentate phosphine ligand, [$Co_2(CO)_6$(μ-$PPh_2C{\equiv}CPPh_2$)], **1**, from the reaction of a bifunctional ligand, bis(diphenylphosphino)acetylene (DPPA), with 1 equiv of $Co_2(CO)_8$ (Scheme 1).[3] Unfortunately, crystallization of **1** was not feasible due to its oily nature.[4] Treatment of **1** with another molar equivalent of $Co_2(CO)_8$ yielded a brown complex, [$Co_2(CO)_4$(μ-CO)$_2${μ-P,P-(μ-$PPh_2C{\equiv}CPPh_2$)$Co_2(CO)_6$}], **2**.

Scheme 1

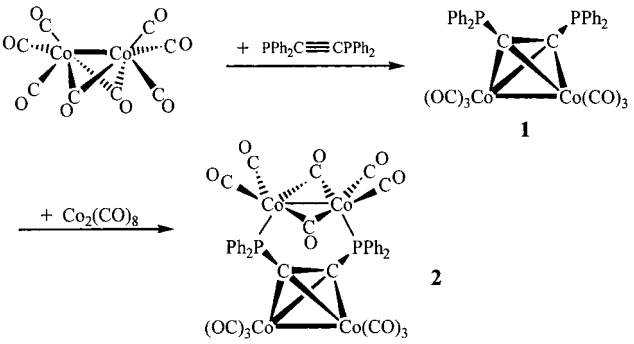

The crystal structure of **2** (Figure 1) shows that the framework consists of a pseudo-tetrahedral Co_2C_2 unit with a bidentate phosphine-bridged Co_2 fragment. Both the $-PPh_2$ substituents are bent away from the DPPA-bridged dicobalt center and coordinate to another dicobalt fragment. The bond angles of P(1)−C(13)−C(14) and P(2)−C(14)−C(13) are 136.56(19)° and 132.32(18)°, respectively. The two cobalt atoms Co(1) and Co(2) and two phosphorus atoms are almost coplanar, with a dihedral angle of 9.39°. In this respect, it can be

* To whom correspondence should be addressed.

(1) (a) Puddephatt, R. J. *Coord. Chem. Rev.* **1980**, *33*, 149. (b) Elliot, D. J.; Holah, D. G.; Hughes, A. N.; Magnuson, V. R.; Moser, I. M.; Puddephatt, R. J.; Xu, W. *Organometallics* **1991**, *10*, 3933. (c) Cornils, B., Herrmann, W. A., Eds. *Applied Homogeneous Catalysis with Organometallic Compounds*; VCH: New York, 1996; Vols. 1, 2. (d) Noyori, R. *Asymmetric Catalysis in Organic Synthesis*; John Wiley & Sons: New York, 1994. (e) Parshall, G. W.; Ittel, S. D. *Homogeneous Catalysis*, 2nd ed.; John Wiley & Sons: New York, 1992; Chapter 8. (f) Vollhardt, K. P. C. *Acc. Chem. Res.* **1977**, *10*, 1. (g) Kagan, H. B. Asymmetric Synthesis Using Organometallic Catalysts. In *Comprehensive Organometallic Chemistry*; Wilkinson, G., Stone, F. G. A., Abel, E. W., Eds.; Pergamon Press: Oxford, 1982; Vol. 8, Chapter 53. (h) Jacobsen, E. N., Pfaltz, A., Yamamoto, H., Eds. *Comprehensive Asymmetric Catalysis*; Springer-Verlag: New York, 1999; Vol. I.

(2) (a) Carty, A. J.; Efraty, A.; Ng, T. W.; Birchall, T. *Inorg. Chem.* **1970**, *9*, 1263. (b) Nickel, T. M.; Yau, S. Y. W.; Went, M. J., *J. Chem. Soc., Chem. Commun.* **1989**, 775. (c) Powell, A. K.; Went, M. J. *J. Chem. Soc., Dalton Trans.* **1992**, 439. (d) Bennett, M. A.; Castro, J.; Edwards, A. J.; Kopp, M. R.; Wenger, E.; Willis, A. C. *Organometallics* **2001**, *20*, 980. (e) Daran, J.-C.; Cabrera, E.; Bruce, M. I.; Williams, M. L. *J. Organomet. Chem.* **1987**, *319*, 239. (f) Hogarth, G.; Norman, T. *Polyhedron* **1996**, *15*, 2859. (g) Bruce, M. I. *Coord. Chem. Rev.* **1997**, *166*, 91.

(3) Hong, F.-E.; Huang, Y.-C.; Wang, S.-L.; Liao, F.-L. *Inorg. Chem. Commun.* **1999**, *2*, 450.

(4) (a) Carty, A. J.; Ng, T. W.; Carter, W.; Palenik, G. J. *J. Chem. Soc., Chem. Commun.* **1969**, 1101. (b) Carty, A. J.; Ng, T. W. *J. Chem. Soc., Chem. Commun.* **1970**, 149.

10.1021/om0106783 CCC: $22.00
Publication on Web 02/07/2002

Scheme 2

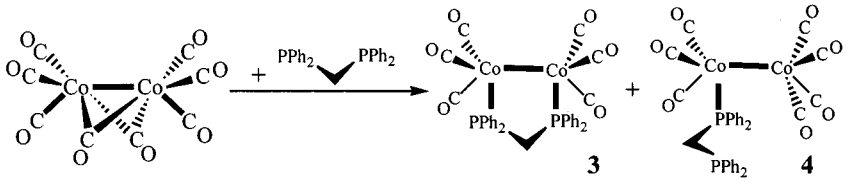

Figure 1. Molecular structure of $[Co_2(CO)_4(\mu\text{-}CO)_2\{\mu\text{-}P,P\text{-}(\mu\text{-}PPh_2C{\equiv}CPPh_2)Co_2(CO)_6\}]$, **2**.

regarded as a modified form of 1,2-bis(diphenylphosphino)ethane (DPPE), a very commonly used bidentate phosphine ligand.[5]

In this work we explored the bonding capacity of the bifunctional ligand $PPh_2C{\equiv}CPPh_2$ toward the dicobalt system. The preparations and reactivities of a series of compounds related to **1** are presented. To improve the crystallization of alkyne-bridged dicobalt compounds, a diphosphine bridging ligand, in this study DPPM, was used. Here we also report the geometric change of the bifunctional ligand $PPh_2C{\equiv}CPPh_2$ after coordination to a dicobalt fragment through its triple bond, which brings about a significant effect upon chelation toward molybdenum carbonyl complex.

Results and Discussion

(A) Synthesis of DPPA-Bridged Dicobalt Carbonyl Complexes. Treatment of DPPM with 1 equiv of $Co_2(CO)_8$ in THF at 60 °C for 8 h afforded two DPPM-coordinated dicobalt compounds, $[Co_2(CO)_6(\mu\text{-}P,P\text{-}PPh_2CH_2PPh_2)]$, **3**, and $[Co_2(CO)_7(\mu\text{-}P\text{-}PPh_2CH_2PPh_2)]$, **4** (Scheme 2).[6]

Further reaction of **3** with DPPA in THF at 45 °C for 5 h produced a DPPA-bridged dicobalt compound $[\{\mu\text{-}P,P\text{-}PPh_2CH_2PPh_2\}Co_2(CO)_4\{\mu\text{-}PPh_2C{\equiv}CPPh_2\}]$, **5** (Scheme 3).

During its chromatographic process, interestingly, two complexes, $[\{\mu\text{-}P,P\text{-}PPh_2CH_2PPh_2\}Co_2(CO)_4\{\mu\text{-}PPh_2C{\equiv}CP(=O)Ph_2\}]$, **6**, with one phosphorus atom oxidized and $[\{\mu\text{-}P,P\text{-}PPh_2CH_2PPh_2\}Co_2(CO)_4\{\mu\text{-}P(=O)Ph_2C{\equiv}CP(=O)Ph_2\}]$, **7**, with two phosphorus atoms oxidized, along with **5**, were obtained. However, compounds **6** and **7** were not present in the crude reaction mixture ^1H NMR. The oxidation must have taken place during the chromatographic separation process, most likely the oxide source being from silica gel. This observation is further supported by the fact that increasing amounts of **6** and **7** were obtained on prolonging the chromatographic separation process purposely. Since this type of oxidation was not observed during the purification process of **1**, it is speculated that the addition of the electron-donating DPPM ligand to the framework of **1** makes the oxidation of the phosphorus atoms more feasible.[7]

Scheme 3

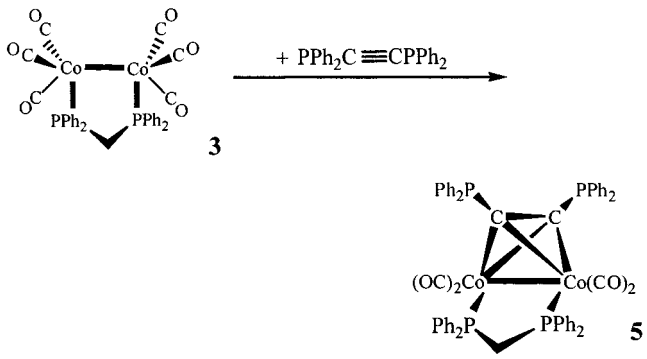

Crystallizations of **5**, **6**, and **7** were successful, which is contrast to the case of **1**, probably due to the addition of the DPPM ligand, and their crystal structures were determined by X-ray diffraction studies. The main frameworks for these three compounds are not much different (Table 2, Figure 2). All carbonyls are terminal. The phenyl rings of the bridged DPPA in all three cases are pointed away from the center of the molecule to prevent steric hindrance. The oxide points down toward the adjacent proton of the methylene in the case of **6** and **7**. The two cobalt atoms and two phosphorus atoms of the DPPM are almost coplanar, as in the case of **2**. The dihedral angles are 9.39°, 12.13°, and 7.08° for **5**, **6**, and **7**, respectively. The bond lengths of the bridged alkynes are 1.344(4), 1.364(5), and 1.359(3) Å for **5**, **6**,

(5) (a) Collman, P.; Hegedus, L. S.; Norton, J. R.; Finke, R. G. *Principles and Applications of Organotransition Metal Chemistry*; University Science Books: Mill Valley, CA, 1987; Chapter 3. (b) Puddephatt, R. J. *Chem. Soc. Rev.* **1983**, *12*, 99.

(6) Lisic, E. C.; Hanson, B. E. *Inorg. Chem.* **1986**, *25*, 812.

(7) Patel, H. A.; Carty, A. J.; Hota, N. K. *J. Organomet. Chem.* **1973**, *50*, 247.

Table 1. Crystal Data of 2, 5, 6, 7, 8, and 9

	2	5	6	7	8	9
formula	$C_{38}H_{20}Co_4O_{12}P_2$	$C_{57}H_{44}Cl_4Co_2O_4P_4$	$C_{55}H_{42}Co_2O_5P_4$	$C_{55}H_{42}Co_2O_6P_4$	$C_{62}H_{42}Co_2O_5P_4Se$	$C_{64}H_{54}Cl_2Co_2MoO_9P_4$
fw	966.20	1176.46	1024.63	1040.63	1187.66	1375.65
temp (K)	293(2)	293(2)	293(2)	293(2)	293(2)	293(2)
cryst syst	triclinic	monoclinic	triclinic	triclinic	triclinic	monoclinic
space group	$P\bar{1}$	$P2(1)/c$	$P\bar{1}$	$P\bar{1}$	$P\bar{1}$	$P2(1)/c$
a (Å)	11.2443(7)	11.8168(8)	11.9109(10)	12.2123(8)	12.802(2)	11.7356(7)
b (Å)	11.4188(7)	12.8713(8)	12.0575(10)	14.3194(9)	14.786(3)	23.6043(14)
c (Å)	16.2488(10)	36.274(2)	18.3823(15)	15.9432(10)	15.657(3)	21.9072(12)
α (deg)	102.9100(10)		73.746(2)	89.4280(10)	106.216(4)	
β (deg)	90.8810(10)	96.2360(10)	89.550(2)	73.5230(10)	94.134(5)	90.9150(10)
γ (deg)	109.7200(10)		74.330(2)	66.4200(10)	99.192(4)	
V (Å^3)	1904.9(2)	5484.6(6)	2433.7(3)	2433.3(3)	2787.9(9)	6067.8(6)
Z	2	4	2	2	2	4
D_c (Mg/m^3)	1.685	1.425	1.398	1.420	1.415	1.506
λ(Mo Kα) (Å)	0.71073	0.71073	0.71073	0.71073	0.71073	0.71073
μ (mm^{-1})	1.858	0.962	0.861	0.864	1.411	0.994
2θ range (deg)	1.29 to 27.94	1.68 to 26.02	2.05to 26.00	1.94 to 26.02	2.25 to 26.10	1.74 to 26.04
no. of obsd reflns ($F>4\sigma(F)$)	5922	8577	6924	7433	2792	9374
no. of refined params	505	658	595	604	667	747
R1[a]	0.0311	0.0477	0.0580	0.0420	0.0892	0.0353
wR2[b]	0.0671	0.1465	0.1503	0.1156	0.1875	0.1087
GoF[c]	0.929	1.118	1.226	0.901	0.874	0.885

[a] $R1 = |\sum(|F_o| - |F_c|)/|\sum F_o||$. [b] $wR2 = \{\sum[w(F_o^2 - F_c^2)^2/\sum[w(F_o^2)^2]\}^{1/2}$; $w = 0.10$. [c] $GoF = [\sum w(F_o^2 - F_c^2)^2/(N_{rflns} - N_{params})]^{1/2}$.

Table 2. Comparison of Selected Structural Parameters of 5, 6, 7, 8, and 9

	5	6	7	8	9
		Bond Lengths (Å)			
Co(1)−Co(2)	2.4775(6)	2.4723(7)	2.4871(5)	2.466(3)	2.4871(5)
C(1)−C(2)	1.344(4)	1.364(5)	1.359(3)	1.358(16)	1.365(4)
C(1)−Co(1)	1.973(3)	1.979(4)	1.972(2)	1.997(12)	1.993(3)
C(1)−Co(2)	1.994(3)	1.972(3)	1.956(3)	1.958(13)	2.007(3)
C(2)−Co(1)	1.973(3)	1.963(4)	1.961(3)	1.954(12)	1.980(3)
C(2)−Co(2)	1.983(3)	1.975(4)	1.956(3)	1.882(13)	1.956(3)
C(1)−P(1)	1.807(3)	1.779(4)	1.780(2)	1.790(14)	1.836(3)
C(2)−P(2)	1.802(3)	1.804(4)	1.780(3)	1.832(14)	1.802(3)
Co(1)−P(3)	2.2368(9)	2.2342(11)	2.2411(7)	2.264(4)	2.2366(8)
Co(2)−P(4)	2.2354(9)	2.2422(11)	2.2415(8)	2.233(4)	2.2482(8)
C(55)−P(3)	1.834(3)	1.828(4)	1.833(3)	1.816(12)	1.836(3)
C(55)−P(4)	1.829(3)	1.833(4)	1.828(3)	1.811(12)	1.831(3)
		Bite Distances (Å)			
P(1),P(2)	4.297	4.201	4.442	4.191	3.275
		Distances (Å)			
O(1)−H(55a)		2.373[a]	2.238[a]	2.162[b]	
		Angles (deg)			
P(1)−C(1)−C(2)	148.7(3)	144.1(3)	144.1(2)	146.1(10)	1179(2)
P(2)−C(2)−C(1)	139.0(3)	139.8(3)	156.3(2)	135.9(11)	125.4(2)
Co(1)−C(1)−Co(2)	77.28(11)	77.48(13)	77.79(9)	77.1(5)	76.91(9)
Co(1)−C(2)−Co(2)	77.55(12)	77.78(13)	78.81(10)	80.0(5)	78.38(10)
C(1)−Co(1)−C(2)	39.84(13)	40.47(14)	40.43(10)	40.2(5)	40.20(11)
C(1)−Co(2)−C(2)	39.51(13)	40.43(14)	40.30(10)	41.4(5)	40.28(11)
P(3)−C(55)−P(4)	109.59(17)	110.4(2)	109.14(13)	109.0(7)	107.91(15)
Co(1)−P(3)−C(55)	109.19(11)	111.17(14)	109.52(9)	107.8(4)	109.04(10)
Co(2)−P(4)−C(55)	110.58(11)	109.80(13)	108.70(9)	109.6(4)	107.47(10)
P(3)−Co(1)−Co(2)	99.55(3)	93.40(3)	97.22(2)	99.20(12)	91.14(2)
P(4)−Co(2)−Co(1)	92.71(3)	99.37(3)	95.15(2)	91.98(12)	99.76(2)

[a] The positions of methylene protons were located. [b] The positions of methylene protons were added.

and **7**, respectively, which are all close to the double bond.[8] The bond length values between two cobalt atoms are very close, i.e., 2.4775(6), 2.4723(7), and 2.4871(5) Å for **5**, **6**, and **7**, respectively.

In the ^{31}P NMR spectra, three sets of signals, in the ratio of 2:1:1, were obtained for all three compounds. The more intense, broad peak was assigned to the two phosphorus atoms, which are chemically equivalent in the coordinated DPPM.[9] The other two sharp peaks were assigned to the two nonequivalent phosphorus atoms of DPPA.

(B) Reaction of Complex 5 with Selenium. The reaction of **5** with 2 molar equiv of selenium powder was carried out in THF at room temperature. Compound **8**, [{μ-P,P-$PPh_2CH_2PPh_2$}$Co_2(CO)_4${μ-P(=O)Ph_2C≡CP(=Se)Ph_2}], with two phosphorus atoms oxidized by oxygen and selenium separately, was characterized by spectroscopic means as well as X-ray diffraction studies.

(8) Dickson, R. S. *Adv. Organomet. Chem.* **1974**, *12*, 323.

(9) The broad peak is due to the coupling between phosphine and its attached cobalt (I = 7/2).

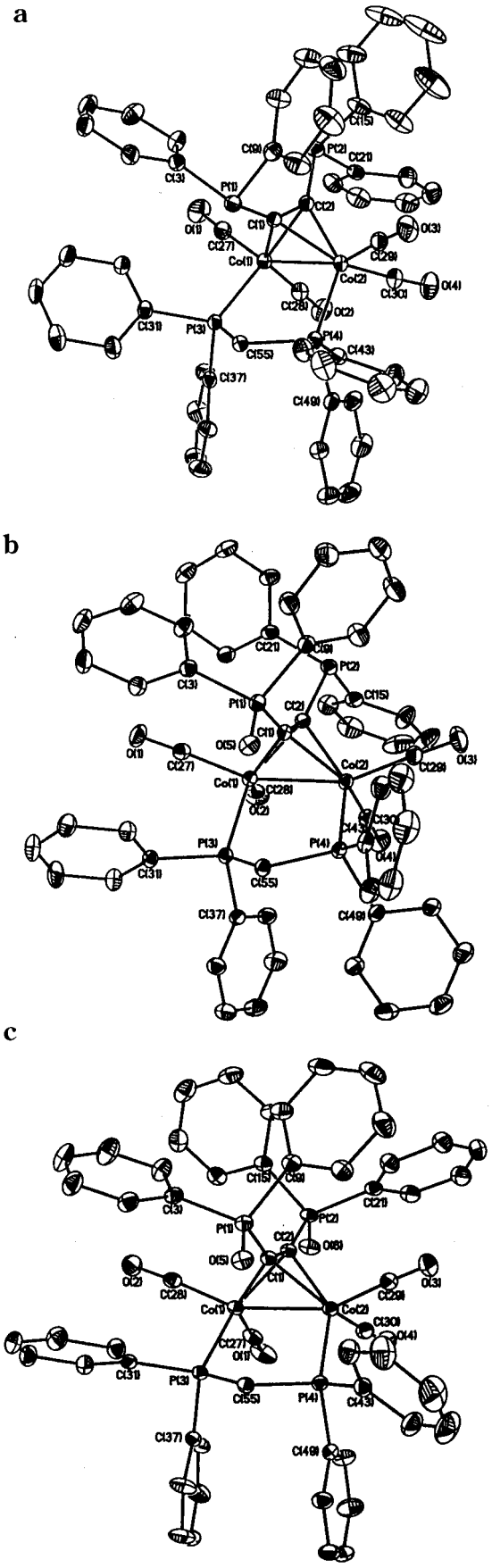

Figure 2. Molecular structures of (a) [{μ-P,P-PPh_2CH_2-PPh_2}$Co_2(CO)_4${μ-$PPh_2C{\equiv}CPPh_2$}], **5**, (b) [{μ-P,P-PPh_2CH_2-PPh_2}$Co_2(CO)_4${μ-$PPh_2C{\equiv}CP(=O)Ph_2$}], **6**, and (c) [{μ-P,P-$PPh_2CH_2PPh_2$}$Co_2(CO)_4${μ-$P(=O)Ph_2C{\equiv}CP(=O)Ph_2$}], **7**.

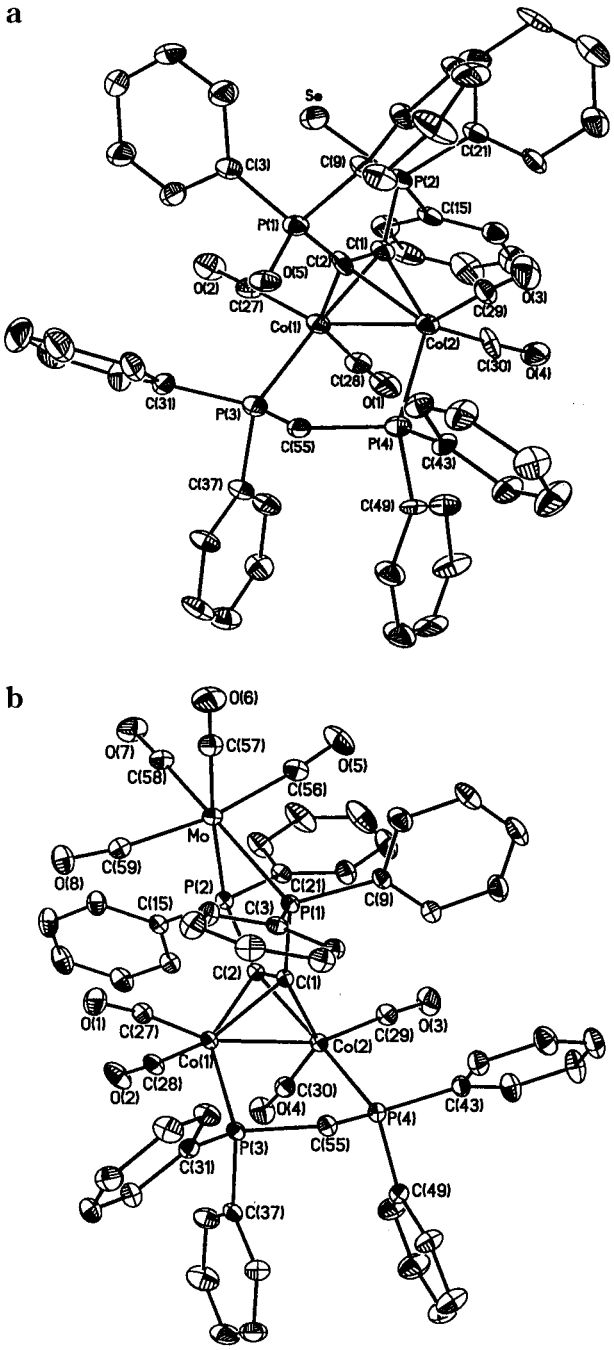

Figure 3. Molecular structures of (a) [{μ-P,P-PPh_2CH_2-PPh_2}$Co_2(CO)_4${μ-$P(=O)Ph_2C{\equiv}CP(=Se)Ph_2$}], **8**, and (b) [{$\mu$-P,P-$PPh_2CH_2PPh_2$}$Co_2(CO)_4${$\mu$-P,P-$PPh_2C{\equiv}CPPh_2$}Mo-$(CO)_4$], **9**.

The oxide of compound **8** is believed to originate from the silica gel during the chromatographic separation process.

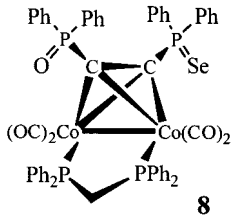

8

The crystal structure of **8** reveals that the distance between the oxide and the adjacent methylene proton,

Scheme 4

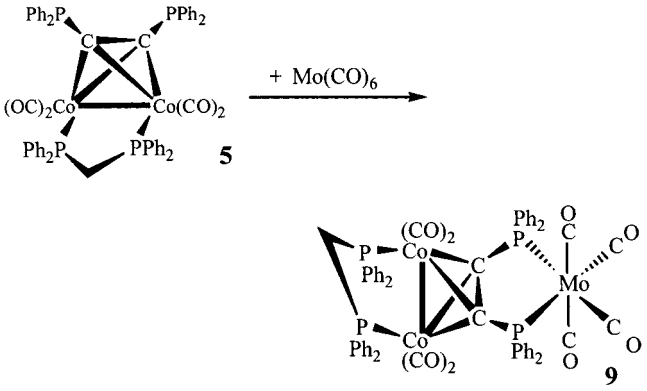

2.162 Å, is well within the range of an intramolecular hydrogen bonding (Table 2, Figure 3).[10] The highly downfield shift of the adjacent methylene proton (6.46 ppm) compared with the remote methylene proton (3.38 ppm) supports this speculation. On the contrary, the selenide is far away from the methylene protons.[11] A C_s symmetry might be designated for this compound in solution state. In ^{31}P NMR, three sets of signals in the ratio of 2:1:1 were obtained. Chemical shifts of all three sets of signals were within the range 30−35 ppm, which is consistent with a coordinated or oxidized phosphorus atom.[12] The ^{31}P−^{77}Se coupling constant of the Se−P bond is 723 Hz, which is consistent with a phosphine having aromatic substituents.[13]

(C) Reaction of Complex 5 with Mo(CO)$_6$. The reaction of **5** with 2 molar equiv of Mo(CO)$_6$ in toluene at 110 °C for 15 h resulted in [(μ-Ph$_2$PCH$_2$PPh$_2$)Co$_2$(CO)$_4$][(μ-P,P-Ph$_2$PC≡CPPh$_2$)Mo(CO)$_4$], **9**, with satisfactory yield (Scheme 4).

Compound **9** was characterized by spectroscopic means as well as X-ray diffraction studies. The structure of **9** can be regarded as a combination of a Mo(CO)$_4$ fragment and **5** (Figure 3). In this regard, **5** behaves as an authentic diphosphine chelating ligand. In contrast with the previous cases, only two sets of peaks in the ratio of 2:2 were observed for **9** in the ^{31}P NMR spectrum at 20 °C. They are peaks at 49.7 and 33.9 ppm for DPPA and DPPM, respectively. The bite angle for P(1)−Mo−P(2) is 79.6°, which is about 3° smaller than average DPPE-chelated complexes and 6° larger than average DPPM-chelated complexes.[14] The dicobalt carbonyl fragment bridges to the triple bond of the DPPA in **5** might indeed narrow the bite angle of the complex.

Selected structural parameters of **5**−**9** are shown in Table 2 for the purpose of comparison. The atom numbering of the main structures of all these compounds has been kept the same.

As shown in Table 2, the main frameworks for these compounds are not much different. Complex **8** has the shortest distance between O(1) and H(55a) among the three compounds **6**, **7**, and **8**, with intramolecular

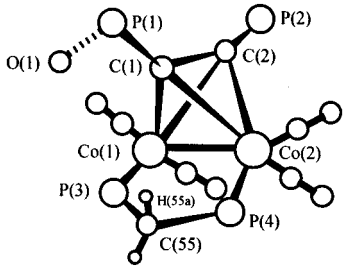

A generalized structure for **5**, **6**, **7**, **8** and **9**

hydrogen bonding. The bite distance between P(1) and P(2) for **9** is much shorter than the others due to its binding to a single metal center.

(D) ^{1}H NMR Variable-Temperature Experiments. Unexpectedly, the ^{1}H NMR of **5** does not show the methylene peaks at room temperature. On the contrary, the corresponding peaks do appear for **6**, **7**, and **8**. It was speculated that the thermal motion of the methyl-

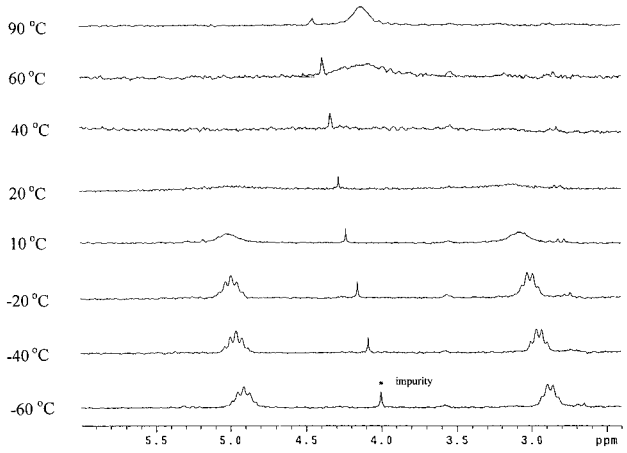

Figure 4. Variable-temperature ^{1}H NMR spectra of **5** in tolene-d_8.

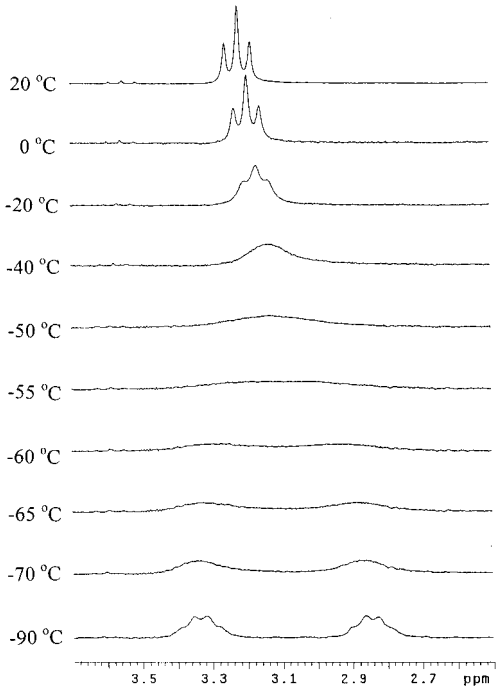

Figure 5. Variable-temperature ^{1}H NMR spectra of **9** in toluene-d_8.

(10) The commonly observed hydrogen bonding ranges from 2.05 to 2.40 Å. Taylor, R.; Kennard, O. *J. Am. Chem. Soc.* **1982**, *104*, 5063.
(11) These distances are 6.855 and 7.970 Å.
(12) Normally, a negative value will be obtained for an uncoordinated phosphine in ^{31}P NMR.
(13) Allen, D. W.; Taylor, B. F. *J. Chem. Soc., Dalton Trans.* **1982**, 51.
(14) Dierkes, P.; van Leeuwen, P. W. N. M. *J. Chem. Soc., Dalton Trans.* **1999**, 1519.

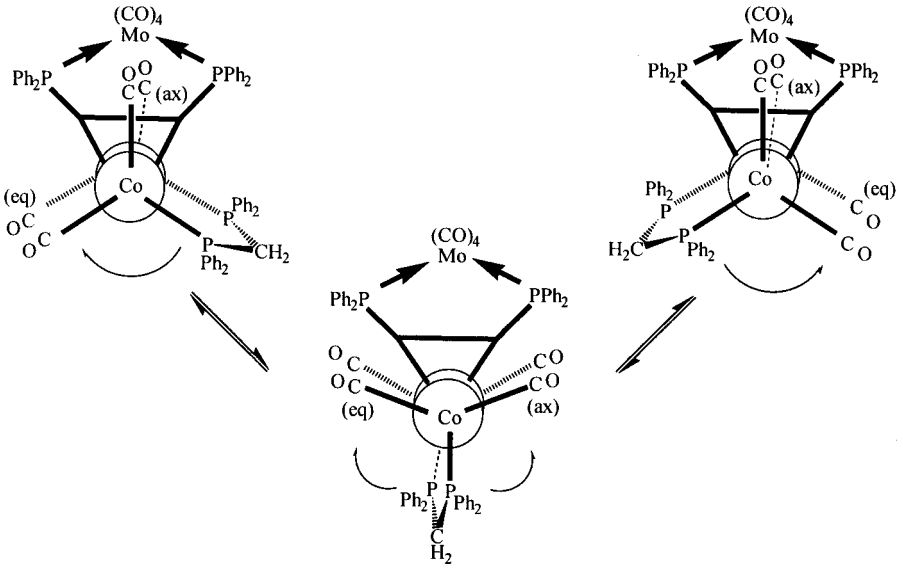

Figure 6. Proposed fluxional behavior of DPPM in **9**.

ene fragment in the DPPM ligand of **5** caused this abnormal phenomenon. The variable-temperature ^{1}H NMR experiment was carried out for **5** in toluene-d_8 over the range −90 to 90 °C. Measurements were taken at intervals of 10 °C (Figure 4). It is clearly seen that the expected methylene peaks do appear at temperatures below 10 °C. When the temperature was raised to 90 °C, two sets of peaks merged into one eventually. The variable-temperature ^{1}H NMR experiments were carried out for **6** and **8** also in the same manner. The appearance of two sets of multiplets did not change even at 90 °C. It was proposed that intramolecular hydrogen bonding was attributed to these observations. The distances of oxygen to the adjacent proton of the methylene are 2.373, 2.238, and 2.162 Å for **6**, **7**, and **8**, respectively, being within the commonly observed hydrogen-bonding range (Table 2, Figures 3−5). It is believed that in the cases of **6**, **7**, and **8** the flexibility of the methylene group, i.e., the up-and-down motions, was limited by the intramolecular hydrogen bonding between the oxide and the adjacent proton of the methylene group, while in the case of **5**, the thermal motion of the methylene group is relatively free and the corresponding methylene protons disappeared, as the coalescence temperature for **5** happened to be near room temperature.[15]

Only one set of triplet signals in the ^{1}H NMR was observed at room temperature for the methylene of DPPM in **9**. A variable-temperature experiment was carried out for **9** similar to the procedures shown above (Figure 5). Two distinct sets of multiplet signals were observed at −90 °C. A mechanism is proposed for the fluxional behavior of DPPM in **9** (Figure 6). It shall work for **5** as well. The back-and-forth motion of the coordinated ligands on the dicobalt fragment might cause a change in the positions of the axial carbonyls with equatorial carbonyls as well as the location of the DPPM. Two methylene protons are equivalent in the fast exchange range, while in the slow exchange range

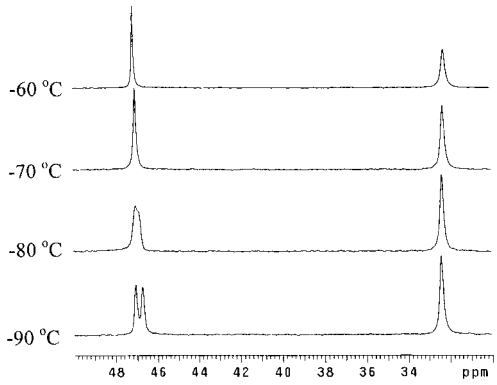

Figure 7. Variable-temperature ^{31}P NMR spectra of **9** in toluene-d_8.

the methylene protons are split. The calculated activation energies from the experiments concerning the fluxional movements of DPPM in **5** and **9** are 19.2 and 7.1 kcal/mol, respectively, at 293 K. The fact that the latter value is much less than the former one indicates that the fluxional motion is much easier in **9**. It is probably because the coordination of the chelating phosphine ligands lessens the steric hindrance between phenyl rings from both DPPM and DPPA.

The fluxional behavior of DPPM in **9** is also evidenced from the variable-temperature ^{13}P NMR (Figure 7). The splitting pattern of two phosphorus signals from DPPA is clearly seen as the measured temperature is lowered to −90 °C.

Summary

In this work, the bonding capacities of the bifunctional ligand $PPh_2C{\equiv}CPPh_2$ toward dicobalt carbonyl complexes were explored. The results show that this ligand could be incorporated into a dicobalt moiety through its triple bond, forming some new, unconventional mono- or bidentate phosphine complexes. In contrast to **6**, **7**, and **8**, the absence of intramolecular hydrogen bonding accounts for the fluxional behaviors of **5** and **9**.

Experimental Section

General Procedures. All operations were performed in a nitrogen-flushed glovebox or in a vacuum system. Freshly

(15) (a) Ebsworth, E. A. V.; Rankin, D. W. H.; Cradock, S. *Structural Methods in Inorganic Chemistry*; Blackwell Scientific: Oxford, 1991. (b) Drago, R. S. *Physical Methods for Chemits*; Saunders: Philadephia, 1992.

distilled solvents were used. All processes of separations of the products were performed by centrifugal thin-layer chromatography (TLC, Chromatotron, Harrison model 8924). ^{1}HNMR spectra were recorded (Varian VXR-300S spectrometer) at 300.00 MHz; chemical shifts are reported in ppm relative to internal TMS. ^{31}P and ^{13}C NMR spectra were recorded at 121.44 and 75.46 MHz, respectively. ^{1}H NMR spectra of variable-temperature experiments were recorded by the same instrument. Some other routine ^{1}H NMR spectra were recorded with a Gemini-200 spectrometer at 200.00 MHz or a Varian-400 spectrometer at 400.00 MHz. IR spectra of solutions in CH_2Cl_2 were recorded on a Hitachi 270-30 spectrometer. Mass spectra were recorded on a JEOL JMS-SX/SX 102A GC/MS/MS spectrometer. Elemental analyses were recorded on a Heraeus CHN-O-S-Rapid.

Synthesis of $Co_2(CO)_4(\mu\text{-}CO)_2(\mu\text{-}P,P\text{-}(\mu\text{-}PPh_2C{\equiv}CPPh_2)Co_2(CO)_6$), 2. Into a 100 cm^3 flask was placed dicobalt octacarbonyl, $Co_2(CO)_8$ (1.00 g, 2.924 mmol), and bis(diphenylphosphino)acetylene (DPPA) (1.153 g, 2.924 mmol) in 30 cm^3 of THF, and the mixture was stirred for 5 h. The brown product was recognized as DPPA-bridged dicobalt compound $Co_2(CO)_6(\mu\text{-}PPh_2C{\equiv}CPPh_2)$, **1**. Further treatment of **1** (1.2 g, 1.764 mmol) with $Co_2(CO)_8$ (0.6 g, 1.755 mmol) in THF at 55 °C for 8 h yielded a brown solution. The solvent was removed, and the resulting residue was chromatographed by CTLC. **2** (22%) was obtained from the brown band eluted by CH_2Cl_2/hexane, 1:1. Crystals were obtained from the CH_2Cl_2/hexane solution of **2** at 4 °C.

Complex 2: brown crystalline solid; ^{1}H NMR ($CDCl_3$, δ/ppm) 7.34−7.59(m, 20H, arene); ^{13}C NMR ($CDCl_3$, δ/ppm) 125.00(s, 2C, C≡C), 128.17(m, 8C, arene), 130.68(s, 4C, *p*-arene), 133.05(m, 8C, arene), 136.37(d, J_{p-c} = 20.1 Hz, 2C, ipso-arene), 136.11(d, J_{p-c} = 20.1 Hz, 2C, ipso-arene), 197.57(m, COs); ^{31}P NMR ($CDCl_3$, δ/ppm) 53.78; IR(CH_2Cl_2) $\nu_{(CO)}$ 1797(sh), 1984(s), 2013(s), 2044(s), 2066(s), 2097(m) cm^{-1}. Anal. Calcd for **2**: C 47.24; H 2.09. Found: C 46.57; H 2.14. MS: 968(M^+ + 2).

Syntheses of $[\{\mu\text{-}P,P\text{-}PPh_2CH_2PPh_2\}Co_2(CO)_4\{\mu\text{-}PPh_2C{\equiv}CPPh_2\}]$, 5, $[\{\mu\text{-}P,P\text{-}PPh_2CH_2PPh_2\}Co_2(CO)_4\{\mu\text{-}PPh_2C{\equiv}CP(=O)Ph_2\}]$, 6, and $[\{\mu\text{-}P,P\text{-}PPh_2CH_2PPh_2\}Co_2(CO)_4\{\mu\text{-}P(=O)Ph_2C{\equiv}CP(=O)Ph_2\}]$, 7. The same procedure described for **2** was followed. The reaction of $Co_2(CO)_8$ with DPPM at 60 °C for 7 h yielded yellow-colored $[Co_2(CO)_6(\mu\text{-}P,P\text{-}PPh_2CH_2PPh_2)]$, **3** (72%), and small amount of green-colored $[Co_2(CO)_7(\mu\text{-}P\text{-}PPh_2CH_2PPh_2)]$, **4**. Further reaction of **3** with DPPA at 45 °C for 5 h produced complex **5**, from which **6** and **7** were isolated during the chromatographic process. The yields for **5**, **6**, and **7** are 53.0%, 17.1%, and 5.7%, respectively.

Complex 5: red crystalline solid; ^{1}H NMR ($CDCl_3$, δ/ppm) 7.13−7.40(m, 40H, arene); ^{13}C NMR ($CDCl_3$, δ/ppm) 127.80−139.03(m, 48C, arene); ^{31}P NMR ($CDCl_3$, δ/ppm) −14.7(1P), 1.2(1P), 31.1(2P); IR (CH_2Cl_2) $\nu_{(CO)}$ 1972(s), 1999(s), 2023(s) cm^{-1}. Anal. Calcd for **5**: C, 65.49; H, 4.20. Found: C, 64.80; H, 4.11. MS(FAB): *m*/*z* 1009(M^+).

Complex 6: red crystalline solid; ^{1}H NMR ($CDCl_3$, δ/ppm): 3.35(q, J_{H-H} = 12.20 Hz, 1H, CH_2), 6.12(q, J_{H-H} = 13.20 Hz, 1H, CH_2), 6.88−7.79(m, 40H, arene); ^{31}P NMR ($CDCl_3$, δ/ppm) 0.81(1P), 27.01(1P), 35.87(2P); IR (CH_2Cl_2) $\nu_{(CO)}$ 1979(m), 2006(s), 2029(m) cm^{-1}. Anal. Calcd for **6**: C, 64.46; H, 4.13. Found: C, 64.07; H, 6.75. MS(FAB): 1025(M^+).

Complex 7: orange crystalline solid; ^{1}H NMR ($CDCl_3$, δ/ppm) 3.32(q, J_{H-H} = 12.60 Hz, 1H, CH_2), 6.10(q, J_{H-H} = 12.80 Hz, 1H, CH_2), 6.86−7.78(m, 40H, arene); ^{13}C NMR ($CDCl_3$, δ/ppm) 128.04(m, 16C, arene), 129.06(s, 4C, *p*-arene), 129.65(s, 4C, p-arene), 131.38(m, 16C, arene), 134.63(d, J_{P-C} = 21.37 Hz, 8C); ^{31}P NMR ($CDCl_3$, δ/ppm) 27.69(1P), 31.48(1P), 35.13(2P); IR (CH_2Cl_2) $\nu_{(CO)}$ 1982(w), 2007(w), 2048(w) cm^{-1}. Anal. Calcd for **7**: C, 63.48; H, 4.07. Found: C, 62.82; H, 4.11. MS(FAB): 1041(M^+).

Syntheses of $[\{\mu\text{-}P,P\text{-}PPh_2CH_2PPh_2\}Co_2(CO)_4\{\mu\text{-}P(=O)Ph_2C{\equiv}CP(=Se)Ph_2\}]$, 8. Into a 100 cm^3 flask was placed $[\{\mu\text{-}P,P\text{-}PPh_2CH_2PPh_2\}Co_2(CO)_4\{\mu\text{-}PPh_2C{\equiv}CPPh_2\}]$ (0.880 g, 0.873 mmol) and selenium (0.138 g, 1.746 mmol) in 15 cm^3 of THF. The solution was frozen by liquid N_2, then the gas was pumped out. The solution was warmed to room temperature and then was stirred for 8 h. The resulting solution was filtered through a small amount of silica gel. The filtrate was evaporated under reduced pressure to yield a crude product. Purification with CTLC was carried out in a 1:1 CH_2Cl_2/hexane mixed solvent. The second eluted dark-red-colored product was identified as **8** in a yield of 73.0% (0.7024 g, 0.637 mmol).

Complex 8: dark red crystalline solid; ^{1}H NMR ($CDCl_3$, δ/ppm) 6.90−8.05(m, 40H, arene), 6.46(m, 1H, CH_2), 3.38(m, 1H, CH_2); ^{13}C NMR ($CDCl_3$, δ/ppm) 25.58(s, 1C), 36.20(t, CH_2), 67.95(s, 1C0, 127.80(m, 16C, arene), 129.17(s, 4C, *p*-arene), 129.75(s, 4C, *p*-arene), 132.39(m, 16C, arene), 134.29(d, J_{P-C} = 9.7 Hz, 8C), 200.15(CO), 205.76(CO); ^{31}P NMR ($CDCl_3$, δ/ppm) 30.31(s, 1P), 33.85(s, 2P), 35.27(d, J_{Se-P} = 723.7 Hz). Anal. Calcd for **6**: C 59.85; H, 3.81. Found: C, 59.09; H, 4.38. MS(FAB): *m*/*z* 1105(P + 1) $^+$.

Syntheses of $[\{\mu\text{-}P,P\text{-}PPh_2CH_2PPh_2\}Co_2(CO)_4\{\mu\text{-}P,P\text{-}PPh_2C{\equiv}CPPh_2\}Mo(CO)_4]$, 9. Complex **5** (0.83 g, 0.82 mmol) was placed in a 100 cm^3 flask along with 2 molar equiv of $Mo(CO)_6$ (0.44 g, 1.65 mmol) in 15 cm^3 of toluene, and the mixture was refluxed for 15 h. The residue was filtered through a small amount of silica gel. Complex **9** was eluted out during the chromatographic process with a solvent mixture of 1:1 CH_2Cl_2/hexane. The yield for **9** was 81.8%.

Complex 9: dark brownish solid; ^{1}H NMR ($CDCl_3$, δ/ppm) 7.01−7.80(m, 40H, arene), 3.21(t, J_{P-H} = 11.1 Hz, −CH_2 of dppm); ^{13}C NMR ($CDCl_3$, δ/ppm) 217.57(dd, one CO of Mo), 211.55(dd, one CO of Mo), 203.51(m, two COs of Mo), 127.87−139.14(m, 48C, arene); ^{31}P NMR ($CDCl_3$, δ/ppm) 33.9(2P of dppm), 49.7(2P of dppa); IR(CH_2Cl_2) $\nu_{(CO)}$ 2012(s), 1905(vs), 1862(s) cm^{-1}. Anal. Calcd for **5**: C, 58.24; H, 3.48. Found: C, 58.41; H, 3.24. MS(FAB): *m*/*z* 1217(P + 1) $^+$.

X-ray Crystallographic Studies. Suitable crystals of **2**, **5**, **6**, **7**, **8**, and **9** were sealed in thin-walled glass capillaries under a nitrogen atmosphere and mounted on a Bruker AXS SMART 1000 diffractometer. The crystallographic data were collected with Mo Kα radiation (λ = 0.71073 Å). Intensity data were collected in 1350 frames with increasing ω (width of 0.3° per frame). The absorption correction was based on the symmetry equivalent reflections using the SADABS program. The space group determination was based on a check of the Laue symmetry and systematic absences and was confirmed using the structure solution. The structure was solved by direct methods using the SHELXTL package. All non-H atoms were located from successive Fourier maps, and hydrogen atoms were refined using a riding model. Anisotropic thermal parameters were used for all non-H atoms, and fixed isotropic parameters were used for H atoms. Crystallographic data of **2**, **5**, **6**, **7**, **8**, and **9** are summarized in Table 1.

Acknowledgment. We are grateful to the National Science Council of the R.O.C. (Grant NSC 89-2113-M-005-026) for financially supporting this research.

Supporting Information Available: Atomic coordinates of **2**, **5**, **6**, **7**, **8**, and **9**, and tables of thermal parameters, bond lengths and angles, anisotropic thermal parameters, and H atom coordinates. This material is available free of charge via the Internet at http://pubs.acs.org.

OM0106783